JETIR.ORG ISSN: 2349-5162 | ESTD Year : 2014 | Monthly Issue
JOURNAL OF EMERGING TECHNOLOGIES AND INNOVATIVE RESEARCH (JETIR)
An International Scholarly Open Access, Peer-reviewed, Refereed Journal

PLANT-MEDIATED GREEN SYNTHESIS OF SILVER NANOPARTICLES USING *RICINUS COMMUNIS* AND *ARTOCARPUS* LEAF EXTRACTS: CHARACTERISATION AND BIOLOGICAL POTENTIAL

[1]Anjana. E, [2]Dr M. Syed Ali, [3]Dr A. Subhashini
[1] PhD Scholar, [2]Assistant Professor and Head of the PG & Research Department of Biotechnology,[3]Associate
Professor and Head, Department of Plant Biology and Plant Biotechnology
[1] Department of Plant Biology and Plant Biotechnology
[1] Quaid-e-Millath Govt. College for Women, Chennai, Tamil Nadu, India
[2] Mohamed Sathak College of Arts and Science, Chennai, Tamil Nadu, India
[3] Quaid-e-Millath Govt. College for Women, Chennai, Tamil Nadu, India

ABSTRACT

The increasing demand for sustainable and environmentally benign methods for nanoparticle production has encouraged the exploration of plant-mediated synthesis as an alternative to conventional chemical approaches. The present study aimed to synthesise silver nanoparticles (AgNPs) using leaf extracts of *Ricinus communis* and *Artocarpus* and to evaluate their physicochemical characteristics and biological activities. The plant extracts were initially assessed for their phytochemical constituents and antioxidant potential, followed by their application in the green synthesis of AgNPs. The synthesised nanoparticles were characterised using UV–Visible spectroscopy and scanning electron microscopy (SEM) analysis. The nanoparticles produced using *R. communis* and *Artocarpus* exhibited average particle sizes of approximately <100 nm, respectively. The biological potential of the synthesised nanoparticles was investigated against the bacterial pathogens *Escherichia coli* and *Klebsiella pneumoniae* , and the findings demonstrate that both plant extracts can serve as effective biological reducing and stabilising agents for AgNP synthesis. The synthesised nanoparticles exhibited promising antimicrobial potential, highlighting their possible applications in biomedical and biotechnological fields. Overall, this study establishes plant-mediated synthesis as a simple, cost-effective, and environmentally sustainable approach for the production of biologically active AgNPs.

Keywords: silver nanoparticles; green synthesis; *Ricinus communis* silver nanoparticles (Ri-AgNP); *Artocarpus* silver nanoparticles (At-AgNP); *Escherichia coli*; *Klebsiella pneumoniae*; phytochemicals; characterization; antimicrobial activity;

INTRODUCTION

Ricinus communis, the castor oil plant, is a member of the genus Ricinus, which is traditionally called the castor bean. Castor seed is the source of castor oil, which has a number of uses. Castor oil is a viscous, pale, yellow, non-volatile and non-drying oil with a bland taste. The seed contains 40-60% oil that is rich in triglycerides, mainly ricinolein a toxic alkaloid ricinine and a very toxic albumen called ricin. The seed coat contains ricin, a poison which is present in lower concentrations throughout the plant. *Ricinus communis* has not only got medicinal value, but it also has great promise in the field of biodiesel production. It is inexpensive and environmentally friendly.

Artocarpus, in the same genus as breadfruit or jackfruit, commonly known as chempedak or cempedak, is a member of the genus Moraceae that contains 50 species of trees. Research on the chemical constituents has isolated several classes of compounds of breadfruit, such as triterpenes and flavonoids. *Artocarpus* is a rich source of prenylated flavonoids. The roots grow on or slightly below the surface of the ground and will often produce a shoot, especially if cut or damaged. The fruits and seeds are a good source of carbohydrates, proteins, and fatty acids. Propagating by seed is not popular as seeds lose viability quickly and the germination percentage is low.

Escherichia coli occurs naturally in the intestine of people and animals. It is the most well-known intestinal bacterium. It is even known as "poo bacterium". The reason that it is well known is mainly due to its role in microbiology. Unlike many other *E.coli* gut microbes, it can also survive foe long time outside the body. It is found in places such as water taps. It has been used in various types of research since 1927. One advantage of is that it divides rapidly. As a result, scientists can culture many generations in a short period of time.

Klebsiella pneumoniae is a Gram-negative, rod-shaped bacillus from the genus *Klebsiella* and family Enterobacteriaceae (Boone et.al., 2001). *K.pneumoniae* is facultatively anaerobic, oxidase –negative and produces acid and gas from lactose. It is an enteric bacterium, noted in the intestinal tract of 5% of healthy humans. It can also reside in the skin and mouth. It causes pneumonia in guinea pigs of both sexes and all ages, although there are few reports of natural infections of this animal species with this organism.

Silver nanoparticles are nanoparticles of silver of size between 1nm to 100nm in size. Commonly used are spherical silver nanoparticles, but diamond, octagonal and thin sheets are also popular. Their extremely large surface area permits the coordination of a vast number of ligands. Silver nanoparticles have unique optical, electrical and thermal properties and are being incorporated into products that range from photovoltaics to biological and chemical sensors. Recent advances in nanoscience and nanotechnology radically changed the way we diagnose, treat and prevent various diseases in all respects of human life. Silver Nanoparticles are (AgNP)s one of the most vital and fascinating nanomaterials among several metallic nanoparticles that are involved in biomedical applications. AgNPs play an important role in nanoscience and nanotechnology, particularly in nanomedicine. Although several noble metals have been used for various purpose, AgNPs have been focused on potential applications in cancer diagnoses and therapy. Additional applications include molecular diagnostics and photonic devices, which take advantage of the novel optical properties of these nanomaterials.

Recently, AgNPs have been frequently used in many textiles, wound dressing and biomedical devices. The size and shape of metal nanomaterials are measured by analytical techniques such as TEM, SEM or AFM. Measuring the aggregation state of the particles require a technique to measure the effective size of the particles in the solution such as dynamic light scattering or analytical disc centrifugation. UV-Vis Spectroscopy is the measurement of the wavelength and intensity of absorption of near-ultraviolet and visible light by a sample. Ultraviolet and visible light are energetic enough to promote outer electrons to higher energy levels. UV-Vis spectroscopy is usually applied to molecules and inorganic ions or molecules and inorganic ions or complexes in solution. The UV-Vis spectra have broad features that are of limited use for sample identification but are very useful for quantitative measurements. Scanning Electron Microscopy is a type of electron microscope that produces images of a sample by scanning the surface with a focused beam of electrons. The electrons interact with atoms in the sample. The electron beam is scanned in a raster scan pattern, and the position of the beam is combined with the intensity of the detected signal to produce an image. The signals used by a scanning electron microscope to produce an image result from interactions of the electron beam with atoms at various depths within the sample.

Due to recent advances in nanotechnology, it is now possible to produce silver at the nanoscale. In addition to their potential electronic and transparent conductor applications, the emergence of nano silver materials in medical products is driving the growth of the nano silver market. Silver nanoparticles are being used in numerous technologies and incorporated into a wide array of consumer products that take advantage of their desirable optical, conductive and antibacterial properties. For Diagnostic purposes, they are used in biosensors and numerous assays where the silver nanoparticle materials can be used as biological tags for quantitative detection. As antibacterial agents, they are used in apparel, footwear, paints, wound dressings, appliances, cosmetics and plastics. For conductive applications, they are used in conductive inks and integrated into composites to enhance thermal and electrical conductivity. In Optical Applications, they are used to efficiently harvest light and for enhanced fluorescence and surface-enhanced Raman Scattering.

Silver nanoparticles are intensively explored nanostructures for unconventional and enhanced biomedical applications. AgNP-based nanosystems and nanomaterials are suitable alternatives for drug delivery. Various physicochemical properties and biological functionalities, including their high antimicrobial efficiency and non-toxic nature, are being researched. There is a significant amount of research data providing the beneficial effects of AgNPs in novel biocompatible and nanostructured materials and devices developed for modern therapeutic strategies.

In this study, we discuss the multifunctional bio-applications of AgNPs, thereby demonstrating their potential use as an antibacterial agent. This preliminary research aimed at the production of AgNPs through a bio-reduction method using *Ricinus communis* and *Artocarpus* leaf extracts. Different types of phytochemicals have been involved in the reduction of silver ions in silver nitrate solution, which led to the formation of silver nanoparticles. The synthesised silver nanoparticles were checked with different analytical approaches, and their antibacterial action was assessed with the help of the disc diffusion method. This could pave the way for

novel future biomedical applications of these silver nanoparticles as well as applications in plant biotechnology. The method of delivering biocontrol agents through a nanoparticle-based delivery system in agriculture has not been explored so far.

2. MATERIALS AND METHODS

2.1. COLLECTION OF LEAVES FROM PLANTS AND PREPARATION OF LEAF EXTRACTS

Fresh leaves of *Ricinus communis* and *Artocarpus* were collected from Porur, Chennai. It was then washed thoroughly 2-3 times with tap water and once with sterile water. 20gm of fresh leaves were finally chopped and added to 300ml of distilled water and stirred at 60^{o}c for 1 hr. After boiling, the mixture was cooled and filtered with Whatman filter paper.

2.2. PHYTOCHEMICAL ANALYSIS OF AQUEOUS LEAVES EXTRACTS

The Phytochemical Screening of leaf extracts were assessed by standard methods (Trease and Evans, 1987; Harborne, 1994). Phytochemical screening was carried out on the leaf extracts to identify the major natural chemical groups such as carbohydrates, tannins, saponins, flavonoids, alkaloids, quinones, glycosides, phenols, terpenoids, cardiac glycosides, coumarins, steroids, phytosteroids, Phlobatannins, Anthraquinones, amino acids, and proteins.

Procedure

- **Flavonoids**

  To 2ml of plant extract, 1ml of 2N Sodium hydroxide is added. Presence of yellow colour.

- **Tannins**

  To 1ml of plant extract, 2ml of 5% Ferric chloride is added.Formation of dark blue or greenish black colour indicates the presence.

- **Carbohydrates**

  To 2ml of plant extract, 1ml of Molish's reagent and few drops of concentrated Sulphuric acid is added. Presence of purple or reddish colour.

- **Saponins**

  To 2ml of plant extract, 2ml of distilled water is added and shaken in graduated cylinder for 15 minutes. Formation of 1cm layer of foam.

- **Alkaloids**

  To 2ml of plant extract, concentrated Hydrochloric acid and few drops of Mayer's reagent is added. Presence of green colour or white precipitat

- **Quinines-** To 0.5ml of plant extract, 2ml of Glacial acetic acid and few drops of 5% Ferric chloride is under layered with 1 ml of concentrated Sulphuric acid. Formation of brown ring at the interface.

- **Terpenoids-** To 0.5ml of plant extract, 2ml of Chloroform and concentrated Sulphuric acid is added. Formation of red brown colour at the interface.

- **Phenols-** To 1ml of plant extract, few drops Phenol Ciocalteau's reagent and few drops of 15% Sodium carbonate is added. Formation of blue or green colour.
- **Coumarins**

To 1ml of plant extract, 1ml of 10% Sodium hydroxide is added. Formation of yellow colour.

- **Steroids**

To 1ml of plant extract, equal volume of Chloroform and few drops of concentrated Chloroform is added.Appearance of brown ring.

- **Phlobatannins**

To 1ml of plant extract, few drops of 2% Hydrochloric acid is added. Appearance of red colour precipitate

- **Anthraquinones**

To 1ml of plant extract, few drops of 10% Ammonium solution is added. Appearance of pink colour precipitate.

- **Phytosteroids**

To 1ml of plant extract, equal volume of Chloroform and few drops of concentrated Sulphuric acid is added. Appearance of bluish brown ring.

- **Amino acids**

To 1ml of plant exteact, 2ml of Millon's reagent is added.

- **Proteins**

To 1ml of plant extract, the test solution is heated in hot water bath.

- **Starch**

To 1ml of plant extract, weak aqueous solution is added.

2.3. ANTIOXIDANT ASSAY OF PLANT LEAF EXTRACTS

- The antioxidant activity was determined by the DPPH assay method following the method introduced by Brand-Williams *et.al.* 1995 with minor modification.
- The capability to scavenge the DPPH radical was calculated using the following equations

$$\text{DPPH Scavenger}(\%) = (Ac - As / A\,c) * 100$$

Where Ac and As are the absorbance of the control and test sample, respectively, after 30 minutes measuring at 517nm

- A linear regression analysis was performed to determine the IC50 value for the sample.

2.4. ESTIMATION OF TOTAL FLAVONOID (TFC)

Total flavonoid content in the extracts (ethyl acetate) was determined using the method described by Sankanaka *et at* 2005. The flavonoid content was determined by the aluminium chloride method using Quercetin as a standard. Extracts and Quercetin were prepared in Ethyl acetate (100ml). 0.1 ml of extract was mixed with 0.9ml of distilled water in test tubes, followed by addition of 75 µl of 5% Sodium nitrate solution. After 6

minutes, 10 µl of 10% Aluminium chloride solution was added and the mixture was allowed to stand for further 5 minutes after which 0.5ml of 1 M sodium hydroxide was added to the reaction mixture. The reaction mixture was brought to 2.5ml with distilled water and mixed well. The absorbance was measured immediately at 510nm using a Spectrometer. A calibration curve was generated using various concentrations of quercetin, and the quercetin equivalent (QE) of the sample was expressed in µl/ml of the extract.

Amount TFC= Sample OD / Standard OD * Respective Amount of extract

2.5. ESTIMATION OF TOTAL TANNINS :

The tannin content in the extract was determined by Folin's Ciocalteu method. 0.1ml of the sample extract containing 1 mg was added to a test tube containing 75ml of distilled water, 0.5 ml of Folin's Ciocalteu reagent, and 1 ml of 35% Sodium carbonate. It was made up to 10 mL with distilled water. This mixture was shaken well and kept at room temperature for 30 minutes. A set of reference standard solutions of tannic acid (20, 40, 60, 80, and 100 µl/mg) was also used. Absorbance for test and standard solutions was measured against the blank at 1725 nm with a UV/Visible Spectrometer. The tannic content was expressed in terms of mg of tannic acid equivalents (TE) µl/ml of the extract.

Amount TTC = Sample OD / Standard OD * Respective Amount of extract

2.6. DETERMINATION OF PHENOLIC CONTENT :

The amount of phenolic compounds in the extracts was determined by the Folin-Ciocalteu calorimetric method and calculated from a calibration curve obtained with Gallic Acid as standard (100 mg/ml).From the standard solution, 20- 100 µl was taken and added to different test tubes. Extract was added in a separate test tube at a concentration of 100 mg/ml and 5ml of Folins-Ciocalteau's(1:10) was added, and the contents were mixed thoroughly. Then, 4 ml of 0.7 M sodium carbonate was added and the mixture was incubated for 30 minutes. The absorbance was measured at 765nm in a UV-Vis Spectrometer. The results were expressed in Gallic acid equivalence of the sample (GE) µl/mg of the extract.

Amount TPC = Sample OD / Standard OD * Respective Amount of extract

2.7. GREEN SYNTHESIS OF SILVER NANOPARTICLES

Green synthesis of silver nanoparticles (AgNPs) was carried out using aqueous leaf extracts of *Artocarpus* and *Ricinus communis* as natural reducing and stabilising agents. Phytochemicals such as phenolic compounds, flavonoids, proteins and other secondary metabolites present in the leaf extracts can reduce Ag^{+} ions from silver nitrate ($AgNO_3$) to elemental silver (Ag^0), resulting in the formation of silver nanoparticles. These phytochemicals can also participate in capping and stabilisation of the nanoparticles.

2.7.1. Preparation of Leaf Extract

1. Fresh and healthy leaves of *Artocarpus* and *R. communis* were collected separately and authenticated before use.
2. The leaves were washed thoroughly with tap water to remove dust and surface contaminants, followed by washing with double-distilled water.

3. The cleaned leaves were air-dried/shade-dried and cut into small pieces.
4. 10 g of fresh leaf material was weighed separately for each plant.
5. Each 10 g sample was crushed using a mortar and pestle and transferred into a conical flask containing 100 mL of double-distilled water.
6. The mixture was heated gently for approximately 10–15 min, with occasional stirring, to extract the water-soluble phytochemicals.
7. The extract was allowed to cool to room temperature.
8. The extract was filtered first through clean filtration material and subsequently through Whatman No. 1 filter paper to obtain a clear plant extract.
9. The filtrates of *Artocarpus* and *R. communis* were collected separately and stored at 4 °C until use.

Aqueous plant extraction by washing, cutting/grinding and heating below approximately 60 °C is commonly reported for plant-mediated AgNP synthesis. A specific *R. communis* study also reports preparing an aqueous extract from 10 g leaves in 100 mL double-distilled water.

2.7.2. Preparation of Silver Nitrate Solution

1. Prepare a 1 mM aqueous $AgNO_3$ solution using double-distilled water.
2. Prepare the solution in an amber bottle or wrap the container with aluminium foil because silver nitrate is light-sensitive.
3. Keep the $AgNO_3$ solution protected from direct light until use.

A 1 mM $AgNO_3$ concentration is widely used in plant-mediated AgNP synthesis, including published protocols using leaf extracts.

2.7.3. Green Synthesis of AgNPs from *Artocarpus* and *Ricinus communis* Leaf Extracts

1. Transfer 90 mL of 1 mM $AgNO_3$ solution into a clean boiling tube.
2. Add 10 mL of the prepared *Artocarpus* and *Ricinus communis* aqueous leaf extract slowly with continuous stirring.
3. Maintain the reaction mixture under continuous magnetic stirring.
4. Incubate the reaction mixture at approximately 40–60 °C for 1–2 h, or continue incubation until a distinct colour change is observed.
5. Initially, the reaction mixture may appear colourless or pale yellow. Formation of AgNPs is generally indicated by the development of a yellowish-brown to brown colour, which results from the surface plasmon resonance of the nanoparticles.
6. Keep a control containing $AgNO_3$ without plant extract under identical conditions.
7. After completion of the reaction, allow the AgNP suspension to cool to room temperature.

Using plant extract with $AgNO_3$ in approximately a 1:9 ratio is consistent with commonly reported green synthesis approaches. A 2025 study specifically demonstrated aqueous *Artocarpus* leaf extract-mediated AgNP synthesis and reported phenolics and flavonoids as important reducing/stabilizing constituents.

2.7.4. Recovery and Purification of Silver Nanoparticles

1. Transfer the synthesized AgNP suspension into centrifuge tubes.
2. Centrifuge at an appropriate high speed according to the laboratory's validated nanoparticle purification protocol.
3. Carefully discard the supernatant containing unreacted compounds.
4. Redisperse the nanoparticle pellet in double-distilled water.
5. Repeat the washing/centrifugation process several times to remove excess plant metabolites and unreacted silver ions.
6. The purified AgNPs may be stored as an aqueous suspension at 4 °C or dried using an appropriate laboratory drying/lyophilization method for further characterization.

Repeated centrifugation and washing with deionized water are commonly used to remove unreacted silver ions and residual plant components from green-synthesized AgNPs.

2.8. Confirmation and Characterisation of AgNPs

The synthesised nanoparticles should be characterised using suitable analytical techniques:

2.8.1. UV Spectrum Analysis of At-AgNP and Ri-AgNP Silver Nanoparticles

UV- Vis spectra were recorded using a UV-Vis Spectrometer UV 1800 (Shimadzu, Japan) between 200 and 800nm. Methanol was used as a blank. The At-AgNP and Ri-AgNP silver nanoparticle extracts were examined under visible and UV light for proximate analysis. For UV-Vis Spectrometer analysis, the At-AgNP and Ri-AgNP silver nanoparticle extracts were centrifuged at 3000 rpm for 10 min and filtered through Whatman No.1 filter paper using a high-pressure vacuum pump. The sample was diluted to 1:10 with the same solvent.

2.8.2. Scanning Electron Microscopy of At-AgNP and Ri-AgNP Silver Nanoparticles

After the synthesis of the silver nanoparticles, the aqueous nanoparticle suspension was used for scanning electron microscopy (SEM) analysis. A small drop of the nanoparticle suspension was carefully placed onto a clean SEM stub and allowed to dry completely at room temperature to ensure complete evaporation of the water. The dried sample was subsequently subjected to SEM analysis using a JEOL JSM-5800LV scanning electron microscope. The analysis was performed at an accelerating voltage of 15 kV and a sample current of 41 µA. The SEM images were obtained to determine the surface morphology, shape, and approximate size distribution of the synthesised silver nanoparticles.

2.9. Collection Of Bacterial Pathogens

MTCC cultures of the bacterial pathogens like *Escherichia coli* and *Klebsiella pneumoniae* were obtained.

2.9.1. Antibacterial Assay: Disc Diffusion Method

Preparing 100 µg/mL AgNP suspension

The formula is:
Concentration = Mass / Volume
Since:
100 µg/mL = 0.1 mg/mL

From 10 mg of dried silver nanoparticles if the Required volume = 10 mg ÷ 0.1 mg/mL = 100 mL, dissolve/disperse 10 mg of dried AgNPs in 100 mL of distilled/deionized water to obtain a starting concentration of 100 µg/mL.

- Antibacterial assay against bacterial pathogens such as *E.coli* and *Klebsiella pneumoniae* was performed by the standard disc diffusion method.
- Agar medium was used to cultivate bacteria. Fresh overnight culture of inoculum (0.1ml) of each culture was spread onto Nutrient Agar (NB) plates.
- Nutrient broth was used, and bacteria were swabbed from fresh cultures using a sterile cotton swab.
- Using a micropipette, the drilled wells were poured with 20µl, 40µl, 60µl and 80µl of the silver nanoparticles.
- Separate wells of *E. coli* and *Klebsiella pneumonia*e were used in the test as a control for comparison.
- The plates were incubated at 37°C overnight. The next day, the inhibition zones around the discs were measured.

2.9.1. Minimum Inhibitory Concentration Assay of At-AgNP and Ri-AgNP Silver Nano particles (Cortes, M. F.

, et al. 2023)

The minimum inhibitory concentration (MIC) of Ri-AgNP and At-AgNP against *Escherichia coli* and *Klebsiella pneumoniae* was determined using a broth microdilution method based on CLSI M07. Each nanoparticle preparation was tested separately against both bacterial strains in triplicate (n = 3). Serial two-fold dilutions of the AgNP preparations were prepared in an appropriate susceptibility-testing broth to obtain a range of test concentrations. A standardised bacterial inoculum was added to the respective wells containing the nanoparticle dilutions. A bacterial growth control without nanoparticles and a sterility control without bacterial inoculum were included. The plates were incubated under the laboratory's validated conditions, after which bacterial growth was assessed by visual observation and/or optical density measurement. The MIC was recorded as the lowest concentration of Ri-AgNP or At-AgNP showing complete inhibition of visible bacterial growth. The experiment was repeated in three independent replicates, and the results were expressed as mean ± standard deviation where appropriate.

3. RESULTS

3.1. Collection Of Leaves from Plant Specimens *Ricinus communis and Artocarpus*

Dried leaves of about 25gm of *Ricinus communis* and *Artocarpus* were collected.

Ricinus communis leaves Artocarpus leaves

Figure 1: Collection Of Plant Leaves.

3.1.1 Preparation of Leaf Extracts

Aqueous leaf extracts were prepared from the fresh leaves of 25gm and was washed with distilled water 300ml. Then it was filtered using Whatman filter paper No. 1, and the filtrate of the aqueous solvent was collected.

Figure 2: Preparation of Leaf Extracts.

3.2 Qualitative Phytochemical Analysis Of Aqueous Leaf Extracts

The aqueous leaf extracts were subjected to preliminary qualitative phytochemical screening to detect the presence of major classes of secondary metabolites. Standard chemical tests were performed for alkaloids, flavonoids, phenols, tannins, saponins, terpenoids, glycosides, steroids, and carbohydrates. The appearance of characteristic colour changes, precipitates, or froth formation was recorded as positive evidence for the respective phytochemical constituents. The results were expressed qualitatively as absent (−), weakly present (+), moderately present (++), or strongly present (+++), based on the intensity of the observed reaction.

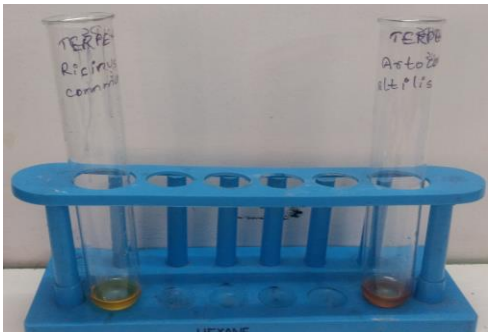

Figure 3: Test for Flavonoids.

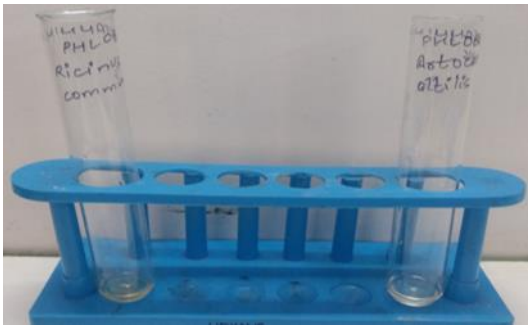

Figure 4: Test for Saponins.

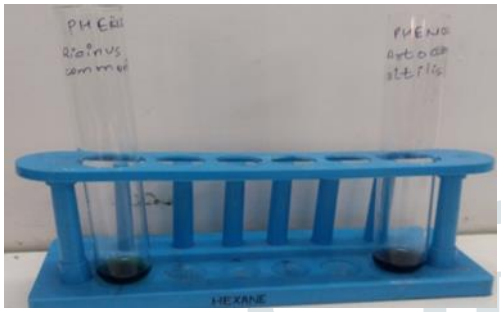

Figure 5: Test for Terpenoids.

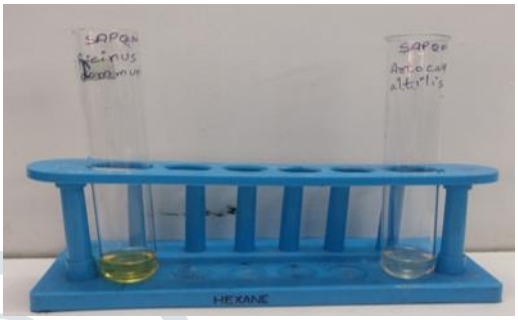

Figure 6: Test for Phlobatannins.

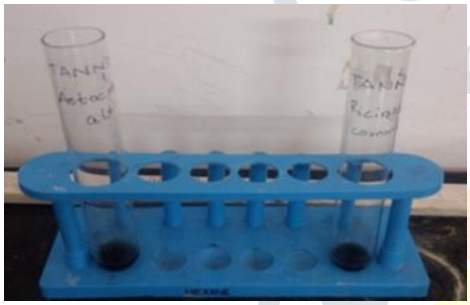

Figure 7: Test for Phenols.

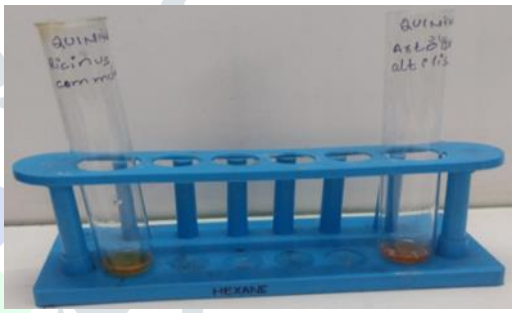

Figure 8: Test for Glycosides

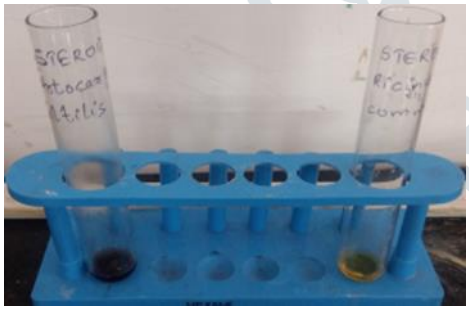

Figure 9: Test for Tannins.

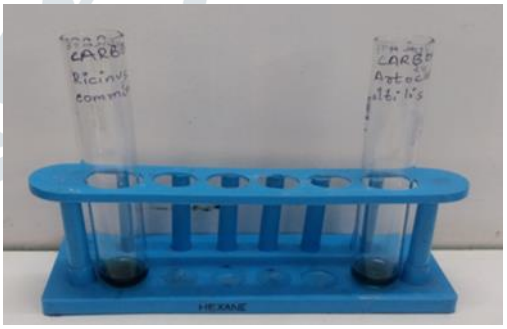

Figure 10: Test for Quinines.

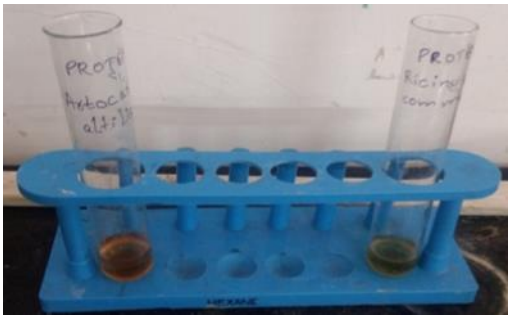

Figure 11: Test for Steroids.

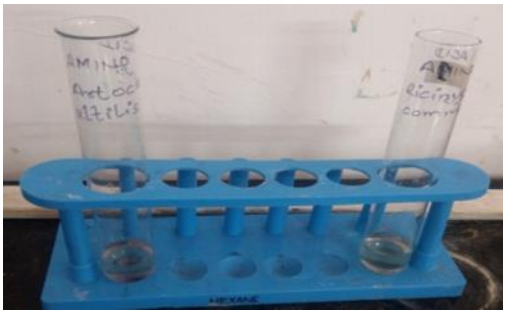

Figure 12: Test for Carbohydrates.

Table 1. Comparative phytochemical screening of *Ricinus communis* and *Artocarpus*

Phytoactive compounds	***Ricinus communis***	***Artocarpus***	**Phytoactive compounds**	***Ricinus communis***	***Artocarpus***
1. Flavonoids	++	--	11. Quinines	+	+
2. Tannins	++	++	12. Cardiac glycosides	--	+
3. Alkaloids	++	++	13. Terpenoids	-	+
4. Glycosides	--	--	14. Coumarins	+	+
5. Proteins	--	--	15. Phytosteroids	-	+
6. Amino acids	--	--	16. Phlobatannins	--	--
7. Carbohydrates	--	--	17. Anthraquinones	-	-
8. Starch	--	--	18. Phenols	++	++
9. Steroids	--	+			
10. Saponins	-	-			

The phytochemical screening results show that *Ricinus communis* and *Artocarpus* contain several bioactive phytochemical constituents, although their profiles differ in some respects.

Ricinus communis showed strong positive reactions (++) for flavonoids, tannins, alkaloids, and phenols, indicating that these compounds are prominent in the tested sample. It also showed positive (+) reactions for quinones and coumarins. Steroids, cardiac glycosides, terpenoids, phytosteroids, and anthraquinones were not detected or showed negative reactions according to the scoring system used.

In contrast, *Artocarpus* showed strong positive reactions for tannins, alkaloids, and phenols, while flavonoids were not detected. It showed positive reactions for steroids, quinones, cardiac glycosides, terpenoids, coumarins, and phytosteroids. Anthraquinones and phlobatannins were not detected.

3.3. Antioxidant Assay of Plant Leaf Extracts

TABLE 2: The antioxidant study conducted on the plant extracts of *Ricinus communis*

C=2.167	200 µl	400 µl	600 µl	800 µl	1000 µl
Ricinus communis	0.141 = 93.49 %	0.116 = 94.64%	0.104 = 95.20 %	0.094 = 95.66 %	0.021 = 94.41 %

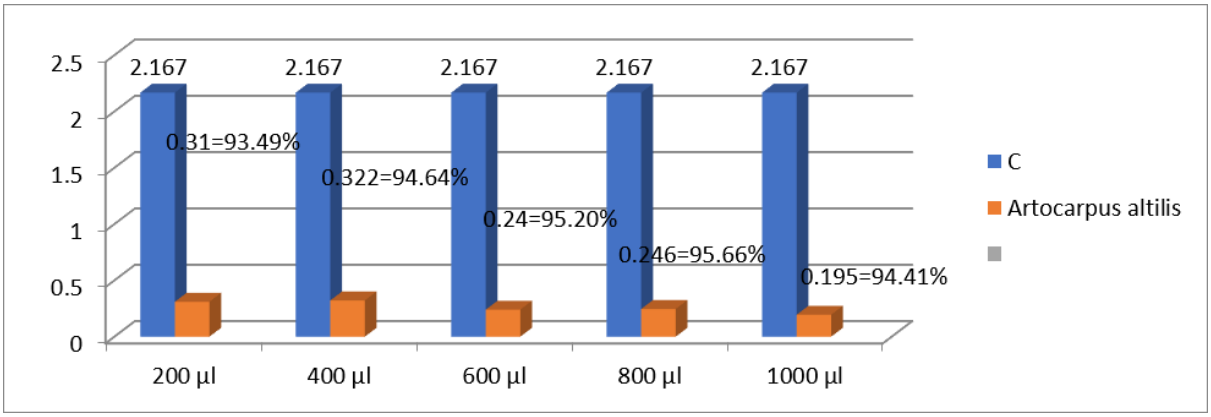

GRAPH 1- Antioxidant assay of *Ricinus* leaf extract

TABLE 3: The antioxidant study conducted on the plant extracts of *Artocarpus*

C = 2.167	200 µl	400 µl	600 µl	800 µl	1000 µl
Artocarpus	**0.310 = 85.69 %**	**0.322 = 85.14 %**	**0.240 = 88.92 %**	**0.246 = 88.64 %**	**0.195 = 91.00 %**

GRAPH 2- Antioxidant assay of *Artocarpus* leaf extract

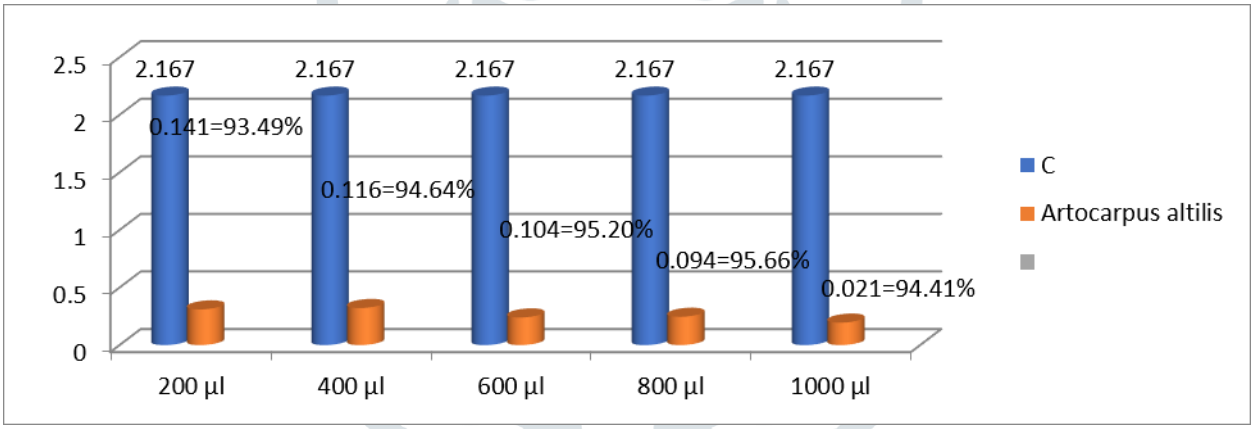

The antioxidant activity of the *Ricinus communis* and *Artocarpus* leaf extracts was evaluated at different concentrations ranging from 200 to 1000 µL. The control/reference absorbance was reported as C = 2.167.

The results indicate that the *Ricinus communis* leaf extract exhibited strong antioxidant activity at all tested concentrations, with inhibition values above 93%. The antioxidant activity increased from 93.49% at 200 µL to 95.66% at 800 µL, accompanied by a progressive decrease in absorbance from 0.141 to 0.094. The graph demonstrates an overall increasing trend in antioxidant activity from 200 to 800 µL, followed by a slight decline at 1000 µL. Thus, under the conditions of this assay, 800 µL showed the highest reported antioxidant activity. The results also demonstrate that the *Artocarpus* leaf extract possesses considerable antioxidant activity, with inhibition values ranging from 85.14% to 91.00%. At 200 µL, the extract exhibited 85.69% antioxidant activity, which decreased slightly to 85.14% at 400 µL. Thereafter, the activity increased to 88.92% at 600 µL, followed by a small decrease to 88.64% at 800 µL. The graph shows that antioxidant activity was relatively stable between 200 and 400 µL, increased at 600 µL, showed a slight reduction at 800 µL, and reached its maximum at 1000 µL. This indicates that the *Artocarpus* extract exhibited its greatest antioxidant effect at the highest concentration tested.

3.4. Estimation Of Total Flavonoid (TFC)

The total flavonoid content of the extracts was measured by the aluminium chloride method in terms of quercetin equivalents (QE). The total flavonoid content present in the sample was estimated as follows.

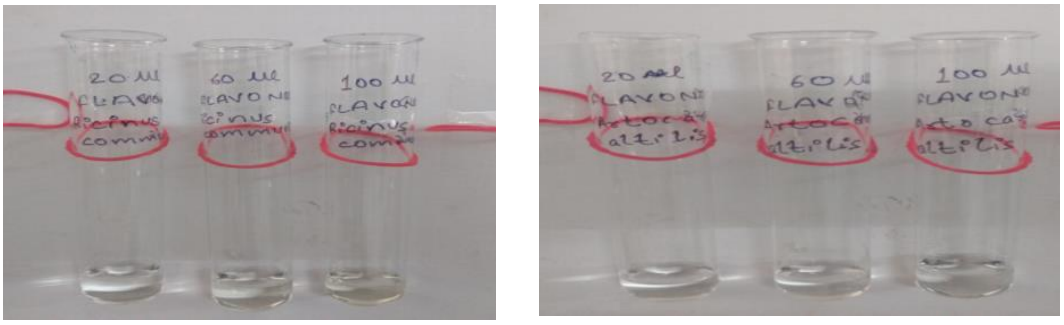

Figure 15-Total Flavonoid Content

TABLE 4 - Estimation of Total Flavonoid Content

Flavonoid Reading	20 µl	60 µl	100 µl
1. *Ricinus communis*	0.082	0.222	0.362
2. *Artocarpus*	-	-	-

GRAPH 3- Total Flavonoid Content

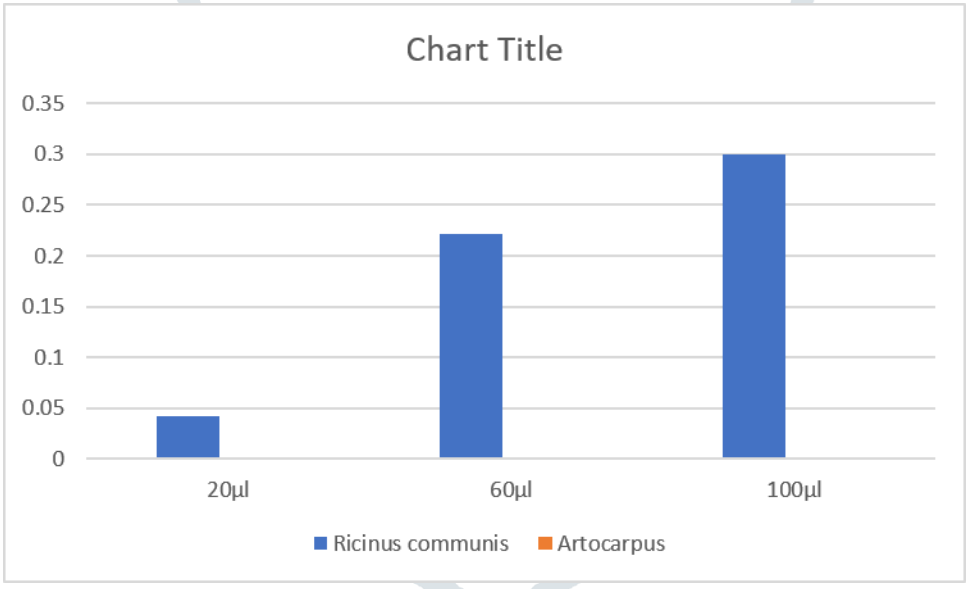

The total flavonoid content of the ethyl acetate extracts of *Ricinus communis* and *Artocarpus* was evaluated using the aluminium chloride colorimetric method, with quercetin used as the standard. Absorbance was measured at 510 nm.

The *Ricinus communis* extract showed detectable flavonoid activity at all three tested volumes. The absorbance increased progressively from 0.082 at 20 µL to 0.222 at 60 µL and 0.362 at 100 µL. This progressive increase in absorbance indicates an increase in the amount of flavonoid-associated reaction product with increasing extract volume.

In contrast, *Artocarpus* showed no detectable response at 20, 60, or 100 µL under the experimental conditions. This indicates that flavonoids were either absent or below the detection limit of the assay in the tested *Artocarpus* extract.

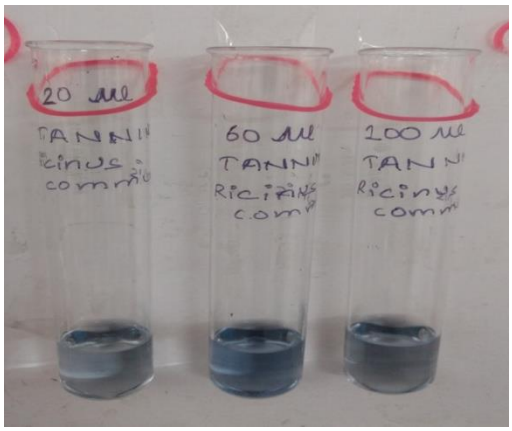

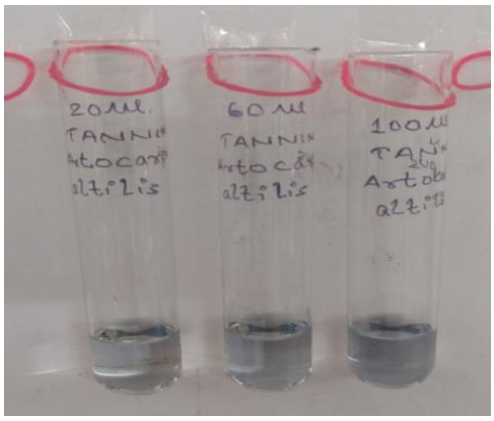

3.5. Estimation Of Total Tannin Content

The total tannin content of the ethyl acetate extracts was determined using the Folin–Denis method and expressed in terms of catechol equivalents (CE). The absorbance of the reaction mixture was measured spectrophotometrically, and the tannin content of the extracts was calculated using the calibration curve prepared with catechol as the standard. The results were expressed as catechol equivalents of the extract.

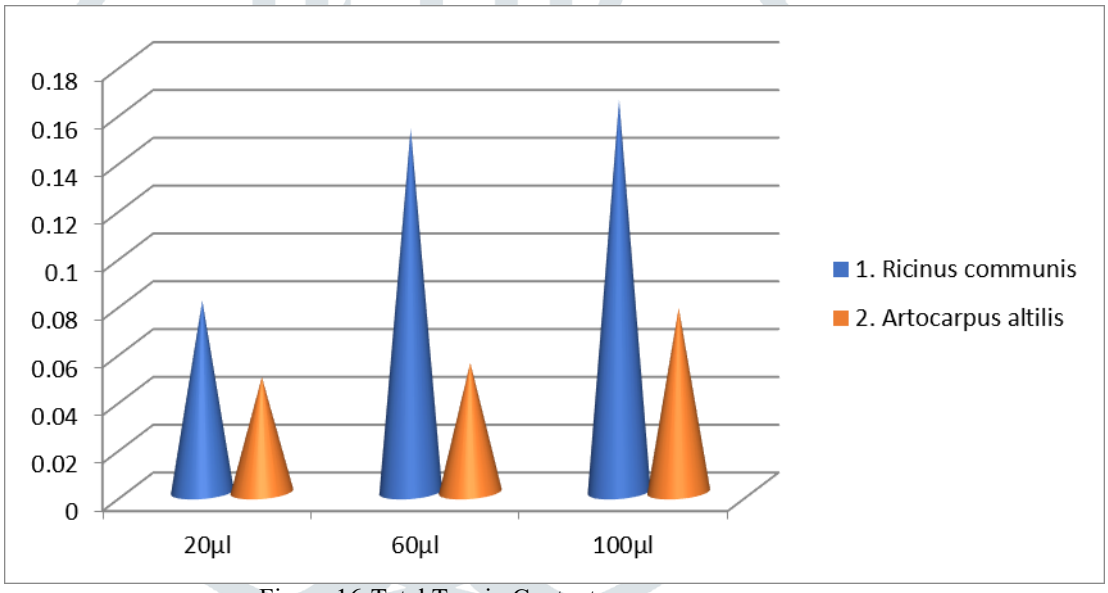

Figure 16-Total Tannin Content

TABLE 5: Estimation of Tannin Content

Tannin Reading	20µl	60µl	100µl
1. *Ricinus communis*	0.080	0.152	0.164
2. *Artocarpus*	0.048	0.054	0.077

GRAPH 4: Total Tannin Content

The results indicate that both *Ricinus communis* and *Artocarpus* extracts contain detectable tannins. *Ricinus communis* showed higher tannin assay readings at all tested extract volumes compared with *Artocarpus*. For *Ricinus communis*, the absorbance increased from 0.080 at 20 µL to 0.152 at 60 µL and 0.164 at 100 µL. Similarly, *Artocarpus* showed an increase from 0.048 at 20 µL to 0.054 at 60 µL and 0.077 at 100 µL.

3.6. Determination Of Phenolic Content

The total phenolic content of the extracts was measured by Folin-Ciocalteu reagents in terms of catechol equivalents (CL) and tabulated. TPC of samples were calculated as shown below

Figure 17: Total Phenolic Content

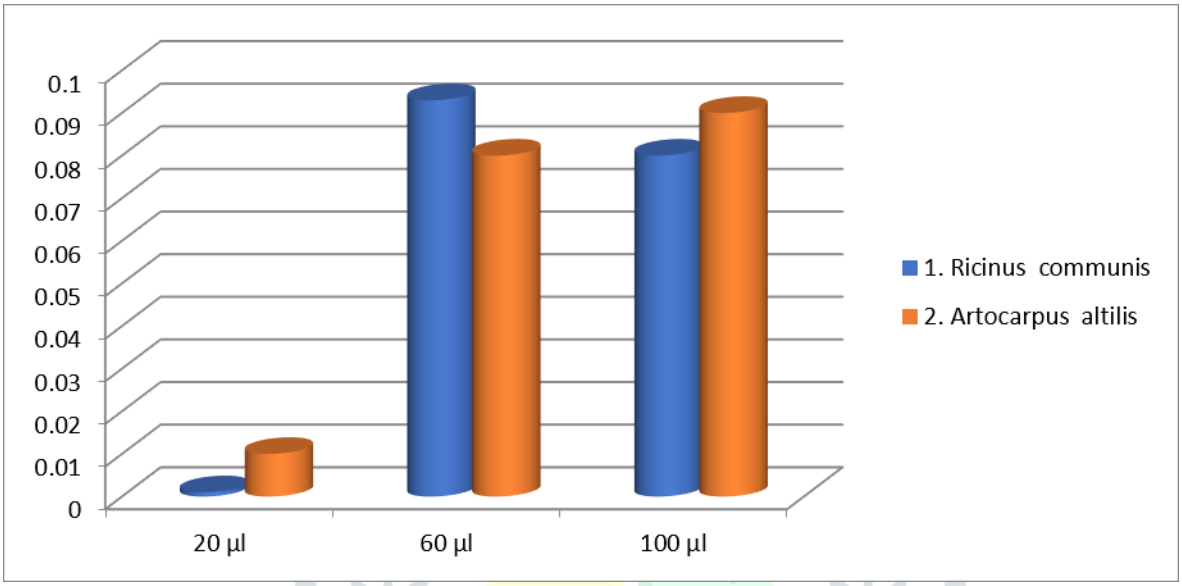

TABLE 6: Estimation of Phenol

Phenol Reading	20 µl	60 µl	100 µl
1. *Ricinus communis*	0.001	0.093	0.080
2. *Artocarpus*	0.010	0.080	0.090

GRAPH 5: Total Phenol Content

The table shows the phenol readings obtained for *Ricinus communis* and *Artocarpus* at three sample volumes (20, 60 and 100 µl).

- *Ricinus communis*: The phenol readings were 0.001, 0.093 and 0.080, respectively. The highest reading was observed at 60 µl (0.093), followed by 100 µl (0.080).

- *Artocarpus*: The readings were 0.010, 0.080 and 0.090, respectively. The highest reading was observed at 100 µl (0.090).

The results indicate that both plant extracts contain phenolic compounds, as shown by their measurable phenol readings. *Ricinus communis* showed its maximum phenol reading at 60 µl, whereas *Artocarpus* showed a gradual increase, reaching its maximum at 100 µl. At 100 µl, *Artocarpus* (0.090) showed a slightly higher reading than *Ricinus communis* (0.080).

2.7. GREEN SYNTHESIS OF SILVER NANOPARTICLES

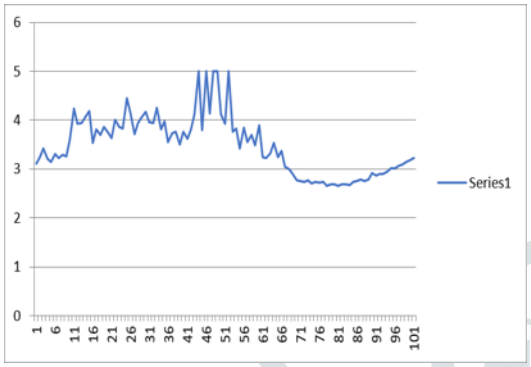

Figure 18: Before Incubation

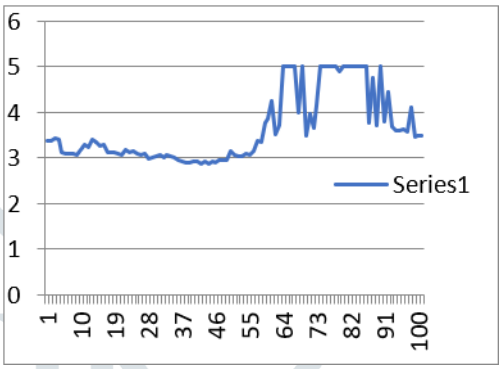

Figure 19: After Incubation

Colour change to Brown from pale yellow indicates the presence of Silver Nanoparticles.

Published *R. communis* studies have demonstrated that its leaf extract can act as both a reducing and capping agent in the formation of AgNPs. One reported protocol used *R. communis* extract with 1 mM $AgNO_3$, while another specifically prepared an aqueous leaf extract using 10 g of leaves in 100 mL of double-distilled water.

2.8. Confirmation and Characterisation of AgNPs

The synthesised nanoparticles were characterised using suitable analytical techniques:

2.8.1. UV Spectrum Analysis of At-AgNP and Ri-AgNP Silver Nanoparticles

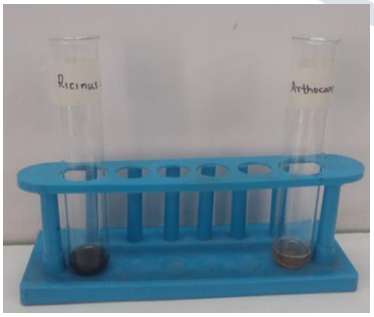

Figure 20:UV Spectrum of At-AgNP

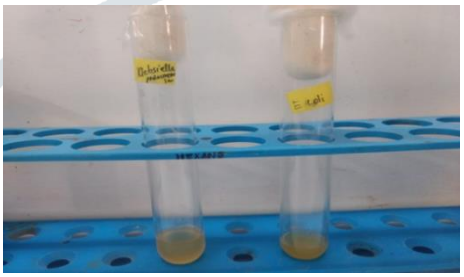

Figure 21: UV Spectrum of Ri-AgNP

The synthesised silver nanoparticles were characterised by UV–Visible spectroscopy to confirm the formation of silver nanoparticles. The UV–Visible spectrum of At-AgNP synthesised using *Artocarpus* leaf extract showed a distinct absorption maximum (λmax) at 415 nm. Similarly, the spectrum of Ri-AgNP synthesised using *Ricinus communis* leaf extract exhibited a characteristic absorption maximum at 420 nm. These absorption peaks in the visible region are attributed to the surface plasmon resonance (SPR) of silver nanoparticles, which results fro

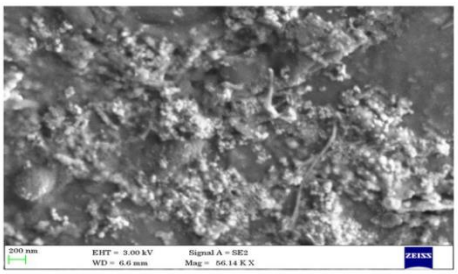

Figure 22: SEM image of Ri-AgNP

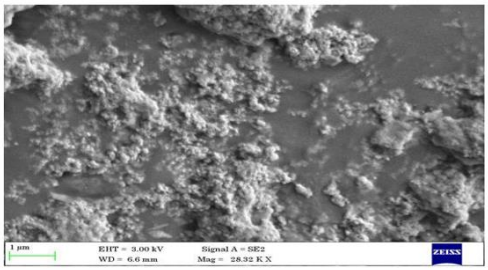

Figure 23: SEM image of At-AgNP

m the collective oscillation of conduction electrons on the surface of the nanoparticles.

2.8.2. Scanning Electron Microscopy of At-AgNP and Ri-AgNP Silver Nanoparticles

Scanning electron microscopy (SEM) was used to evaluate the surface morphology, shape, and size of silver nanoparticles synthesised using *Ricinus communis* (Ri-AgNP) and *Artocarpus* (At-AgNP) leaf extracts. The SEM micrographs revealed the successful formation of silver nanoparticles with well-defined morphological features. The synthesised nanoparticles were predominantly observed in the nanoscale range, with particle sizes below 100 nm, confirming the formation of nanoparticles of suitable dimensions.

2.9. Collection Of Bacterial Pathogens

The MTCC cultures of *Escherichia coli* and *Klebsiella pneumoniae* were revived aseptically by transferring the cultures into appropriate sterile nutrient medium and incubating under the recommended conditions until visible growth was obtained. The revived cultures were then maintained on suitable agar medium for further antibacterial studies.

Figure 24: Revival of the Bacterial Cultures

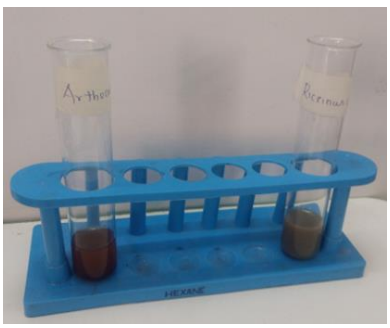

2.9.1. Antibacterial Assay: Disc Diffusion Method

The antibacterial study was conducted on the silver nanoparticles by means of the agar well-diffusion technique against two oral pathogens, namely *Escherichia coli* and *Klebsiella pneumoniae*. Tetracycline was taken as a control for antibacterial studies. The results are shown below. The concentration of the Silver Nanoparticle suspension used was 100 µg/mL.

Figure 25: Inhibition Zones of Ri-AgNP against *E.coli*

TABLE 7: Antibacterial Activity of Ri-AgNP against *E.coli*

Organism	Sample Concentration(100µg/ml)	Zone of Inhibition	
		Sample	Control
E.coli	20µl	10mm	14mm
E.coli	40µl	13mm	14mm
E.coli	60µl	13mm	14mm
E.coli	80µl	14mm	14mm

Figure 26: Inhibition Zones of At-AgNP against *E.coli*

TABLE 8: Antibacterial Activity of At-AgNP against *E.coli*

Organism	Sample Concentration(100µg/ml)	Zone of Inhibition	
		Sample	Control
E.coli	20µl	8mm	14mm
E.coli	40µl	10mm	14mm
E.coli	60µl	10mm	14mm
E.coli	80µl	11mm	14mm

Figure 27: Inhibition Zones of Ri-AgNP against *Klebsiella pneumoniae*

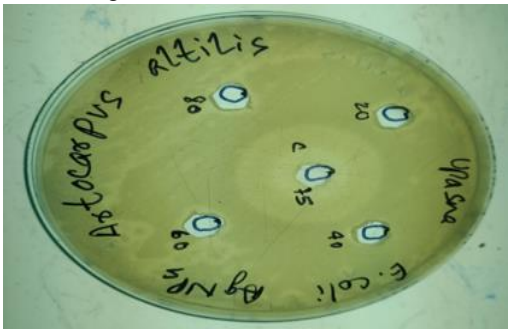

TABLE 9: Antibacterial Activity of Ri-AgNP against *Klebsiella pneumoniae*

Organism	Sample Concentration(100µg/ml)	Zone of Inhibition	
		Sample	Control
K.pneumoniae	20µl	10mm	12mm
K.pneumoniae	40µl	12mm	12mm
K.pneumoniae	60µl	12mm	12mm
K.pneumoniae	80µl	12mm	12mm

Figure 28: Inhibition Zones of At-AgNP against *Klebsiella pneumoniae*

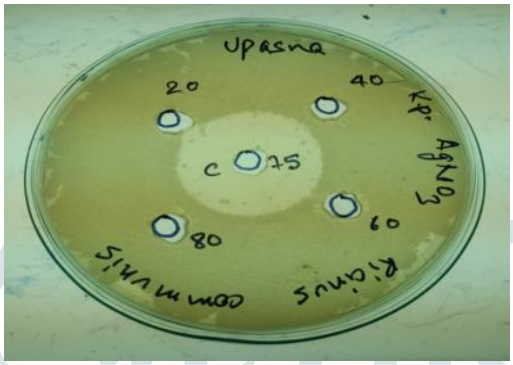

TABLE 10: Antibacterial Activity of At-AgNP against *Klebsiella pneumoniae*

Organism	Sample Concentration(100µg/ml)	Zone of Inhibition	
		Sample	Control
K.pneumoniae	20µl	9mm	12mm
K.pneumoniae	40µl	12mm	12mm
K.pneumoniae	60µl	12mm	12mm
K.pneumoniae	80µl	12mm	12mm

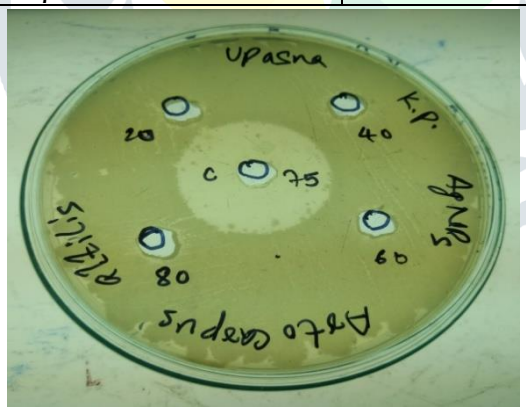

The antibacterial activity of Ri-AgNP and At-AgNP was evaluated against *Escherichia coli* and *Klebsiella pneumoniae* using different sample volumes (20–80 µL) of the 100 µg/mL nanoparticle suspension. Against *E. coli*, Ri-AgNP produced inhibition zones of 10, 13, 13 and 14 mm, while At-AgNP produced zones of 8, 10, 10 and 11 mm at 20, 40, 60 and 80 µL, respectively. Thus, Ri-AgNP showed comparatively greater antibacterial activity against *E. coli* than At-AgNP.

Against *K. pneumoniae*, Ri-AgNP produced inhibition zones of 10, 12, 12 and 12 mm, whereas At-AgNP produced zones of 9, 12, 12 and 12 mm at the respective sample volumes. Both nanoparticles therefore demonstrated antibacterial activity against *K. pneumoniae*, with Ri-AgNP showing slightly greater inhibition at 20 µL and comparable activity at higher volumes.

2.9.1. Determination of Minimum Inhibitory Concentration of At-AgNP and Ri-AgNP Silver Nanoparticles against *E.coli* and *Klebsiella pneumoniae*

TABLE 11: Minimum Inhibitory Assay of *Artocarpus* and *Ricinus communis* AgNPs

Bacterial Strain	Nano-particle	Replicate	100µl (10µg/ml)	80µl (8µg/ml)	60µl (6µg/ml)	40µl (4µg/ml)	20µl (2µg/ml)	Final MIC
E.coli	At-AgNP	R_1	-	-	+	+	+	80µl
		R_2	-	+	+	+	+	100µl
		R_3	-	-	+	+	+	80µl
	Ri-AgNP	R_1	-	-	-	+	+	60µl
		R_2	-	-	-	+	+	60µl
		R_3	-	+	+	+	+	100µl
Klebsiella pneumoniae	At-AgNP	R_1	-	+	+	+	+	100µl
		R_2	-	-	+	+	+	80µl
		R_3	-	-	-	+	+	60µl
	Ri-AgNP	R_1	-	-	-	+	+	60µl
		R_2	-	-	+	+	+	80µl
		R_3	-	-	-	+	+	60µl

The minimum inhibitory concentration (MIC) assay was performed to evaluate the antibacterial activity of At-AgNP and Ri-AgNP against *Escherichia coli* and *Klebsiella pneumoniae*. The assay was carried out in three replicates using nanoparticle concentrations ranging from 2 to 10 µg/mL. A negative (−) result indicated inhibition of visible bacterial growth, whereas a positive (+) result indicated bacterial growth.

For *E. coli*, At-AgNP showed MIC values of 8, 10 and 8 µg/mL in replicates R1, R2 and R3, respectively. Ri-AgNP showed MIC values of 6, 6 and 10 µg/mL, respectively. Thus, Ri-AgNP exhibited comparatively stronger inhibitory activity against *E. coli*, with a lower overall MIC range of 6–10 µg/mL, compared with 8–10 µg/mL for At-AgNP.

Against *K. pneumoniae*, At-AgNP showed MIC values of 10, 8 and 6 µg/mL for R1, R2 and R3, respectively. Ri-AgNP showed an MIC of 6 µg/mL in all three replicates, demonstrating consistent inhibitory activity.

Therefore, Ri-AgNP showed greater and more consistent antibacterial activity against *K. pneumoniae* than At-AgNP.

GRAPH 6: MIC Assay of At-AgNP and Ri-AgNP

4. DISCUSSION

Phytochemical screening revealed that both *Ricinus communis* and *Artocarpus* contained tannins, alkaloids,

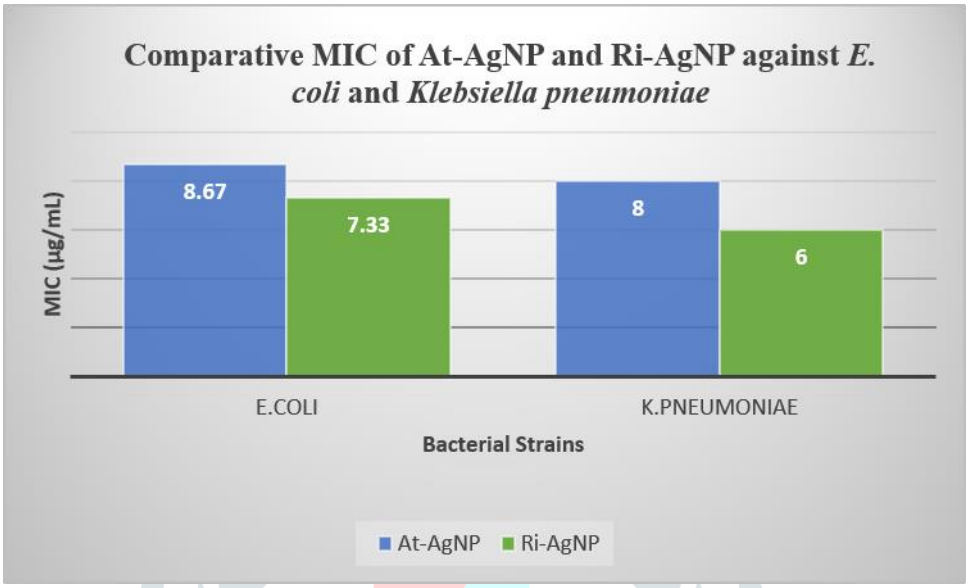

quinones, coumarins, and phenols, while *R. communis* showed a notable presence of flavonoids. In contrast, *Artocarpus* exhibited additional detection of steroids, cardiac glycosides, terpenoids, and phytosteroids. These secondary metabolites may contribute to the antioxidant and antimicrobial properties of the plant extracts and may also help reduce and stabilise silver nanoparticles.

The antioxidant assay demonstrated considerable activity in both extracts. *R. communis* exhibited the higher maximum activity of 95.66% at 800 µL, compared with 91.00% at 1000 µL for *Artocarpus*, indicating comparatively stronger antioxidant potential in *R. communis* under the conditions tested. The flavonoid assay further showed a concentration-dependent increase in *R. communis*, with absorbance increasing from 0.082 to 0.362, whereas no detectable flavonoid response was observed for *Artocarpus*. Similarly, tannin content was higher in *R. communis* than in *Artocarpus*, with maximum absorbance values of 0.164 and 0.077, respectively, at 100 µL. These findings support the contribution of phenolic and other secondary metabolites to the observed antioxidant potential.

The total phenol assay showed that *R. communis* produced its highest reading at 60 µL (0.093), while *Artocarpus* showed its maximum at 100 µL (0.090). The presence of phenolic compounds in both extracts supports their potential role as reducing and stabilising agents during green nanoparticle synthesis.

Successful formation of silver nanoparticles was confirmed by UV–Visible spectroscopy, with characteristic surface plasmon resonance peaks at 415 nm for At-AgNP and 420 nm for Ri-AgNP. SEM analysis further

confirmed the formation of well-defined nanoparticles with particle sizes below 100 nm. The observed nanoscale dimensions and morphology indicate effective bioreduction and stabilisation of silver nanoparticles by phytochemicals present in the respective leaf extracts.

Both nanoparticle preparations demonstrated antibacterial activity against *Escherichia coli* and *Klebsiella pneumoniae*. Ri-AgNP generally produced larger inhibition zones than At-AgNP, particularly against *E. coli*. In the MIC assay, Ri-AgNP showed MIC values of 6–10 µg/mL against *E. coli* and a consistent MIC of 6 µg/mL against *K. pneumoniae*. At-AgNP showed MIC values of 8–10 µg/mL against *E. coli* and 6–10 µg/mL against *K. pneumoniae*. These findings indicate that both green-synthesised AgNPs possess antibacterial potential, with Ri-AgNP showing comparatively greater and more consistent activity under the experimental conditions.

Overall, the findings demonstrate that *R. communis* and *Artocarpus* leaf extracts are promising biological resources for the green synthesis of silver nanoparticles. The combination of phytochemical constituents, antioxidant properties, nanoscale particle formation, and antibacterial activity supports their potential for further investigation as plant-based nano-biocontrol agents.

5. CONCLUSION

The present study demonstrated the potential of *Ricinus communis* and *Artocarpus altilis* leaf extracts for the green synthesis of silver nanoparticles. Both plants contained several biologically important secondary metabolites, while *R. communis* exhibited comparatively higher flavonoid and tannin responses and greater antioxidant activity. The formation of At-AgNP and Ri-AgNP was confirmed by UV–Visible spectroscopy, with characteristic SPR peaks at 415 and 420 nm, respectively, and by SEM, which revealed nanoparticles below 100 nm. Both nanoparticle preparations exhibited antibacterial activity against *E. coli* and *K. pneumoniae*, with Ri-AgNP showing comparatively stronger activity, particularly against *K. pneumoniae*, where a MIC of 6 µg/mL was consistently observed. The findings provide a basis for exploring plant-mediated silver nanoparticles as potential biocontrol agents in sustainable agriculture. Future studies should evaluate their efficacy against important agricultural bacterial and fungal pathogens under greenhouse and field conditions, together with detailed assessment of phytotoxicity, environmental persistence, effects on beneficial soil microorganisms, and nanoparticle–plant interactions. Further research could focus on developing controlled delivery systems, such as nano formulations, biodegradable polymeric carriers, encapsulated formulations, seed-coating systems, foliar sprays, and targeted soil-delivery systems. Such approaches could improve the stability, controlled release, targeting, and field efficacy of nanoparticle-based biocontrol agents while reducing unnecessary application and environmental exposure. Optimisation of dosage, formulation stability, delivery method, and large-scale production will be essential before practical agricultural application. Integration of these nano-enabled biocontrol systems with existing integrated pest and disease management strategies may contribute to the development of more effective and sustainable crop-protection technologies.

7. REFERENCES

1. Abou El-Nour, KM, Eftaiha A, Al-Warthan A, Ammar RA. Synthesis and applications of silver nanoparticles. Arab. J. Chem. 2010. 3, 135-140.

2. Ahamed M, Karns M, Goodson M, Rowe J, Hussain SM, Schager JJ, Hong Y. DNA damage response to different surface chemistry of silver nanoparticles in mammalian cells. Toxicol. Appl. Pharmacol. 2008, 233, 404-410.

3. Albanese A, Tangs PS, Chan WC. The effect of nanoparticle size, shape and surface chemistry on biological systems. Annu. Biomed. Eng. 2012, 14, 1-16. [CrossRef][Pubmed].

4. American Cancer Society. Cancer Facts and Figures 2015. American Cancer Society. Atlanta, GA, USA, 2015.

5. Cabral M, Pedrosa F, Margarido F, Nougueria CA.f-life Zn-MnO2 batteries : Electrode and ZnO-EG nanofluid. J. Exp. Nanosci. 2013, 8, 567-577.

6. Carlson C, Hussain SM, Schrand AM, Brayich-Stolle LK, Hess KL, Jones RL, Schlager JJ. Unique cellular interaction of silver nanomaterials. Size-dependent generation of reactive oxygen species. J. Phys. Chem B. 2008, 112, 13608-13619. [CrossRef][Pubmed].

7. Cator CR. Techniques of the study of Biological Structure and Function; Schimmel PR, Ed, WH Freeman: San Francisco, CA, USA.

8. Chernousova S, Epple M. Silver as antibacterial agent; Ion, nanoparticle and metal. Angew.Chem.Int.Ed. 2013,52, 1636-1653. [Cross Ref] [PubMed]

9. Diane Ragone. Breadfruit – *Artocarpus altilis.* Exotic fruits, 53-60, 2018.

10. David V. Goeddel, Elizabeth Yelverton, Axel Ulrich. Human leukocyte interferon produced by *E. coli* is biologically active. Nature 287(5781), 411, 1980.

11. Deepak V, Umamaheshwara PS, Guhan K, Nanthini RA, Krithiga B, Jaithoon NM, Gurunathan S. Synthesis of gold and silver nanoparticles using purified URAK. Colloid Surface B. 2001, 86, 353-358.

12. Duan XP, Li YP. Physicochemical characteristics of silver nanoparticles affect circulation, biodistribution, cellular internalisation and trafficking. Small 2013, 9, 1521-1532. [Cross Ref][PubMed].

13. Elsupikhe RF, Shameli K, Ahmad MB, Ibrahim NA, Zaiinudun N. Green sonochemical synthesis of silver nanoparticles at varying concentrations of k-carrageenan. Nanoscale Res. Lett. 2015, 10, 302.

14. Enos Tangke Arung, Britanto Dani Wicaksono, Yohana Ayuprivanti Handoko, Irawan Wiiava. Anticancer properties of diethyl ether extract of wood from sukun (*Artocarpus altilis)* in human breast cancer T47D). Tropical Journal of Pharmaceutical Research 8(4), 2009.

15. Gul, A., Fozia, Shaheen, A., Ahmad, I., Khattak, B., Ahmad, M., Ullah, R., Bari, A., Ali, S. S., Alobaid, A., Asmari, M. M., & Mahmood, H. M. (2021). Green synthesis, characterisation, enzyme inhibition, antimicrobial potential, and cytotoxic activity of plant-mediated silver nanoparticles using *Ricinus communis* leaf and root extracts. *Biomolecules, 11*(2), 206. https://doi.org/10.3390/biom11020206

16. Gurav AS, Koda TT, Wang LM, Kauppinen EI, Joutsensaari J. Generation of nanometer size fullerence particles via vapour condensation. Chem. Phys. Lett. 1994, 218, 304-308. [CrossRef][Pubmed].

17. Gurunathan S, Han J, Park JH. A green chemistry approach for synthesizing biocompatible gold nanoparticles. Nanoscale Res. Lett. 2014, 9, 248.

18. Gurunathan S, Han JW, Dayen AA, Eppakayala V, Park JH, Cho SG, Lee KJ, Kim JH. Green synthesised silver nanoparticles and their potential cytotoxicity in human breast cancer cells. Ind. Eng. Chem. 2013, 19, 1600-1605.

19. Gurunathan S, Han JW, Kim ES, Park JH, Kim JH. Reduction of graphene oxide by resveratrol. A novel and simple biological method for the synthesis of an effective anticancer nanotherapeutic molecule. Int.J. Nanomed. 2015, 10, 29512969. [Cross Ref] [PubMed]

20. Gurunathan S, Kalishwaralal K, Vaidyanathan R, Venkataraman D, Pandian SR, Muniyandi J, Hariharan N, Eom SH. Biosynthesis, purification and characterisation of silver nanoparticles using *E.coli*. Colloids Surf. B Interfaces 2009, 74, 328-335. [Cross Ref] [PubMed].

21. Gurunathan S, Lee K, Kalishwaralal K, Sheikhprababu S, Vaidyanathan R, Eom SH. Antiangiogenic properties of silver nanomaterials. Biomaterials 2009, 30, 6341-6350. [CrossRef][Pubmed].

22. Gurunathan S, Park J.H, Han J.W, Kim J.H. Comparative assessment of the apoptotic potential of silver nanoparticles synthesised by *Bacillus tequilensis* and *Calocybe indica* in MDA-MB-231human breast cancer cells, targeting p53 or anticancer therapy. Int. J.Nanomed. 2015, 10, 4203-4222 [Cross Ref] [Pub Med]

23. Gurunathan S. Biologically synthesised silver nanoparticles enhance antibiotic activity against Gram-negative bacteria. J.Ind. Eng. Chem. 2015, 29. 217-226..

24. Jame P Nataro, James B Kaper. Diarrheagenic *Escherichia coli*. Clinical Microbiology Reviews 11(1), 142-201, 1998.

25. Jo DH, Kim JH, Lee TG. Size, surface charge and shape determine therapeutic effects of nanomaterials on brain and retinal diseases. Nanomedicine 2015, 1603-1611. [Cross Ref][PubMed].

26. Kalaishwaralal K, Deepak V, Ramkumarpandian S, Nelliah H, Sanglilyandi G. Extracellular biosynthesis of silver nanoparticles by the culture supernatant of *Bacillus licheniformis.* Mater. Lett. 2008, 62, 4411-4413.

27. Kalishwaralal K, BarathManiKanth S, Pandian SR, Deepak V, Gurunathan S. Silver nanoparticles impede the biofilm by *Pseudomonas aeruginosa* and *Staphycoccus epidermiss.* Colloid Surface B, 2010, 79, 340-344

28. Kim KJ, Sung WS, Moon SK, Choi JS, Lee DG. Antifungal effect of silver nanoparticles on dermatocytes. J. Microbiol. Biotechnol. 2008, 18, 1482-1484.

29. Kruis FE, Fissan H, Rellighanus B. Sintering and evaporation characteristics of gas-phase synthesis of size-selected PbS nanoparticles. Mater. Sci. Eng. B 2000, 69, 329-334. [Cross Ref] [PubMed].

30. Leung TC, Wong CK, Xie Y. Green synthesis of silver nanoparticles using biopolymers, carboxymethylated-curdlan and fucoidan. Matter. Chem. Phys. 2010, 402-405.

31. Li CY, Zhang YJ, Chen G, Li l, Wu D, Wang Q. In vitro real-time visualisation of tissue blood flow and angiogenesis using Ag2S quantum dots in the NR-II window. Biomaterials 2014, 35, 393-400. [Cross Ref] [PubMed]

32. Li L, Hu J, Yang W, Alivisatos AP. Band gap variation of size- and shape-controlled colloidal CdSe quantum rods. Nano Lett. 2001, 1, 349-96. [Cross Ref] [PubMed].

33. Li, W.R., Xie X.B., Shi Q.S., Zeng H.Y., Ou-Yang, Y.S., Chen, Y.B. Antibacterial activity and mechanism of silver nanoparticles on *Escherichia coli*. Appl. Microbial. Biotechnol. 2010,8,1115-1122. [Cross-Ref] [PubMed]

34. Lin J, Huang Z, Wu H, Zhou W, Jin P, Wei P, Zhang F, Zhang J, Xu J. et al. Inhibition of autophagy enhances the anticancer activity of silver nanoparticles. Autophagy 2014, 10, 2006-2020.

35. Lin PC, Lin S, Wang PC, Sridhar R. Techniques for physicochemical characterisation of nanomaterials. Biotech. Adv. 2014, 32, 711-726. [Cross Ref] [PubMed].

36. Link S, Ei-Sayed MA. Optical properties and ultrafast dynamics of metallic nanocrystals. Annu. Rev. Phys. Chem. 2003, 54, 331-336.

37. Gul, A., Fozia, Shaheen, A., Ahmad, I., Khattak, B., Ahmad, M., Ullah, R., Bari, A., Ali, S. S., Alobaid, A., Asmari, M. M., & Mahmood, H. M. (2021). Green synthesis, characterisation, enzyme inhibition, antimicrobial potential, and cytotoxic activity of plant-mediated silver nanoparticles using *Ricinus communis* leaf and root extracts. *Biomolecules, 11*(2), 206. https://doi.org/10.3390/biom11020206

38. Magnussuon MH, Deppert K, Malm JO, Bovin JO, Samuelson L. Size-selected gold nanoparticles by aerosol technology. Nanostruct. Mater. 1999, 12, 45-48. [Cross Ref][PubMed].

39. Mukherjee P, Ahmad A, Mandal D, Senapati S, Sainkar S.K., Khan M.I, Renu P, Ajay Kumar P.V. Alam, M Kumar R et al. Fungus-mediated synthesis of silver nanoparticles and their immobilisation in the mycelia matrix. A novel biological approach to nanoparticle synthesis. Nano Lett. 2001, 1, 515-519 [Cross-Ref][PubMed]

40. Murdock RC, Braydich-Stolle L, Schlager jj, Hussain SM. Characterisation of nanomaterial dispersion in solution before in vitro exposure using dynamic light scattering technique. Toxicol. Sci. 2008, 101-239-253. [Cross Ref] [PubMed].

41. Ogar A, Tylko G, Turnau K. Antifungal properties of silver nanoparticles against indoor mould growth. Sci. Total Environ. 2015, 521, 305-314.

42. Okafor, F., Janen, A., Kukhtareva, T., Edwards, V., & Curley, M. (2013). Green synthesis of silver nanoparticles, their characterisation, application and antibacterial activity. *International Journal of Environmental Research and Public Health, 10*(10), 5221–5238. https://doi.org/10.3390/ijerph10105221

43. Panacek A, Kolar M, Vecerova R, Prucek R, Soukupova J, Krystof V, Hamal P, Zbioril R, Kvitek L. Antifungal activity of silver nanoparticles against Candida spp. Biomaterials 2009, 6333-6340. [Cross Ref] [PubMed].

44. Piao MJ, Kang KA, Lee IK, Kim S, Choi JY, Hyun JW. Silver nanoparticles induce oxidative cell damage in human liver cells through inhibition of reduced glutathione and induction of mitochondria-involved apoptosis. Toxicol. Lett. 2011, 201, 92-100.

45. Pleus R, Nanotechnologies-Guidance on physicochemical Characterisation of Engineered Nanoscale Materials for Toxicologic Assessment, ISO: Geneva, Switzerland, 2012.

46. Plyum T, Powell Q, Gaurav A, Ward T, Kodas T, Glicksman H. Solid silver particle production by spray pyrolysis. J. Aerosol Sci. 1993, 24, 383-392.

47. R. Ilavarasan M, Mallika S, Venkateshwara. Anti-inflammatory and free radical scavenging activity of *Ricinus communis* root extract. Journal of Ethnopharmacology, 2006, 103(3), 478-480.

48. Salem Basha, Kandasamy, Kandasamy Ulaganathan. Antagonism of *Bacillus* species strain (BC121) towards *Curvularia lunata.*

49. Sapsford KE, Tyner KM, Dair BJ, Deschamps JR, Meintz IL. Analysing nanomaterial bioconjugates. A review of current and emerging purification and characterisation techniques. Anal. Chem. 2011, 83,, 4453-4488. [Cross Ref][PubMed].

50. Schmidt Ott A. New approaches to in situ characterisation of ultrafine agglomerates. J Aerosol Sci. 1988, 19, 553-563. [Cross Ref] [PubMed].

51. Shameli K, Ahmad MB, Yunus WM, Rustaiyan A, Ibrahim NA, Zargar M, Abdollahi Y. Green synthesis of silver/montmorrillonite/chitosan bionanocomposites using UV radiation method and evaluation of antibacterial activity. Int. J. Nanomed. 2010, 5, 875-887.

52. Shameli K, Ahmad MB, Yunus WMZW, Ibramin NA, Gharayebi Y, Sedaghat S. Synthesis of silver/montmorillonite nanocomposites using γ-irraadiation. Int. J. Nanomed. 2010. 10, 302.

53. Sharma VK, Yngard RA, Lin Y. Silver nanoparticles: Green synthesis and their antimicrobial activities. Adv. Colloid Interface 2009, 145, 83-96. [Cross Ref] [PubMed].

54. Shivakumar and M. B. Patil. 2023. "Morphological Variability of the *Curvularia Lunata* Associated with Grain Discolouration of Rice". *International Journal of Plant & Soil Science* 35 (21):921-28. https://doi.org/10.9734/ijpss/2023/v35i214062.

55. Sondi I, Salopek –Sondi B. Silver nanoparticles as antibacterial agents. A case study on *E. coli* as a model for quantum dots. Nano Lett. 2001, 1, 349-351 [Cross Ref] [PubMed]

56. Sriram MI, Kanth SBM, Kalaishwaralal K, Gurunathan S. Antitumour activity of silver nanoparticles in Dalton's lymphoma ascites tumour model. Int. J. Nanomed. 2010, 5, 753-762.

57. Staquicini FI, Owaza MG, Moya CA, Driessen WH, Barbu EM, Nishimori H, Soghonnyan S, Flores LG, Liang X, Paolillo V, et al. Systematic combinatorial peptide selection yields a non-canonical iron-mimicry mechanism for targeting tumours in a mouse model of human glioblastoma. J. Chin. Investig. 2011, 121, 161-173. [CrossRef][Pubmed].

58. Sushmita Kaushik, Jagat Ram, A Chakarbarty, MR Dogra Gangadeep S Brar. *Curvularia lunata* endophthamitis with secondary keratis. American Journal of Ophthalmology 13(1), 140-142, 2001.

59. Tao A, Sinsermuksakul P, Yang P. Polyhedral silver nanocrystals with distinct scattering signatures. Angew. Chem. Int. Ed. 2006, 45, 4597-4601.

60. Tien DC, Laio CY, Huang JC, Tsung TT, Kao WS, Tsai TH, Chang TW, Yu BS. Novel technique for preparing a nano-silver water suspension by the arc-discharge method. Rev. Adv. Mater. Sci. 2008, 18, 750-75.

61. Tsuji M, Hashmoto M, Nishiazawa Y, Kubokawa M, Tsuji T. Microwave-assisted synthesis of metallic nanostructures in solution. Chem. Eur. J. 2005, 11, 440-452.

62. UV/VIS/IR Spectroscopy Analysis of Nanoparticles, 2012. Available online: http:'//50.87.149.212/sites/default/file/nanocomposix%20Guidelines%20UV-vis%20Analysis. Pdf.

63. Vanlalveni, C., Lallianrawna, S., Biswas, A., et al. Green synthesis of silver nanoparticles using plant extracts and their antimicrobial activities: a review of recent literature. *RSC Advances*. 2021; 11:2804–2837.

64. Waseda Y, Matsurba E, Shinoda K. X-ray diffraction crystallography: Introduction, Examples and Solved Problems; Springer Verlag; Berlin, Germany, 2011.

65. Wiley B, Sun Y, Mayers B, Xia Y. Shape-controlled synthesis of metal nanostructures. The case of silver. Chemistry 2005, 11, 454-463.

66. Wong KK, Chenug SO, Huang L, Niu J, Tao C, Ho CM, Che, Tam PK. Further evidence of the anti-inflammatory effects of silver nanoparticles. Chem Med Chem. 2009, 4, 1129-1135. [CrossRef][Pubmed].

67. Ze-Quang, Wei, Xiao-Xing Du, Yun-Song Yu, Ping Shen, Ya Gang. Plasmid-mediated KPC-2 in a *Klebsiella pneumoniae* isolate from China. Antimicrobial Agents and Chemotherapy 51(2), 763-765, 2007.

68. Zodrow K, Brunet L, Mahendra S, Li D, Zhang A, Li Q, Alvarez PJ. Polysulfone ultrafiltration membranes impregnated with silver nanomaterials show improved biofouling resistance and virus removal. Water Res. 2009, 43, 715-723. [Cross Ref] [PubMed].